

---

# Multi-modal Self-Supervision from Generalized Data Transformations

---

Mandela Patrick<sup>1,2\*</sup>   Yuki M. Asano<sup>2\*</sup>   Ruth Fong<sup>2</sup>   João F. Henriques<sup>2</sup>  
Geoffrey Zweig<sup>1</sup>   Andrea Vedaldi<sup>1,2</sup>

<sup>1</sup> Facebook AI Research  
mandelapatrik@facebook.com

<sup>2</sup> Visual Geometry Group, University of Oxford  
yuki@robots.ox.ac.uk

## Abstract

Self-supervised learning has advanced rapidly, with several results beating supervised models for pre-training feature representations. While the focus of most of these works has been new loss functions or tasks, little attention has been given to the data transformations that build the foundation of learning representations with desirable invariances. In this work, we introduce a framework for multi-modal data transformations that preserve semantics and induce the learning of high-level representations across modalities. We do this by combining two steps: inter-modality slicing, and intra-modality augmentation. Using a contrastive loss as the training task, we show that choosing the right transformations is key and that our method yields state-of-the-art results on downstream video and audio classification tasks such as HMDB51, UCF101 and DCASE2014 with Kinetics-400 pretraining.

## 1 Introduction

Self-supervised pretraining of image representations has been maturing rapidly and is now competitive with manual supervision while utilizing only raw images with no manually-specified labels. Recent examples include contrastive methods such as PIRL [37], MoCo [19] and SimCLR [57] as well as clustering-based ones such as SeLa [67]. These methods still underperform direct supervised learning when it comes to learning semantic concepts such as object classes, but are entirely comparable to supervised learning for pretraining a representation that is *transferred* to another task.

The main idea behind all these approaches is to learn image representations which are *invariant* to irrelevant nuisance factors in the data while being *distinctive* to the relevant factors. Remarkably, albeit unsurprisingly, these are the same design criteria of traditional computer vision representations such as SIFT [34]. In the absence of an external task such as image classification for supervision, an algorithm cannot tell which factors are relevant or irrelevant. As a proxy, authors have thus modelled irrelevant factors as random *photo-geometric* data transformations, often also called augmentations. Then, the self-supervised learning task is to distinguish images up to these random transformations.

Another line of work in self-supervision uses multiple data modalities instead of using only images. In this case, the task is to predict one modality from the other, such as predicting properties of the audio track in a video from images extracted from it [43]. Cross-modal self-supervision is, in practice, also very powerful, although in these cases, data augmentations have been considered as useful but not key elements of the formulations.

---

\*Joint first authors

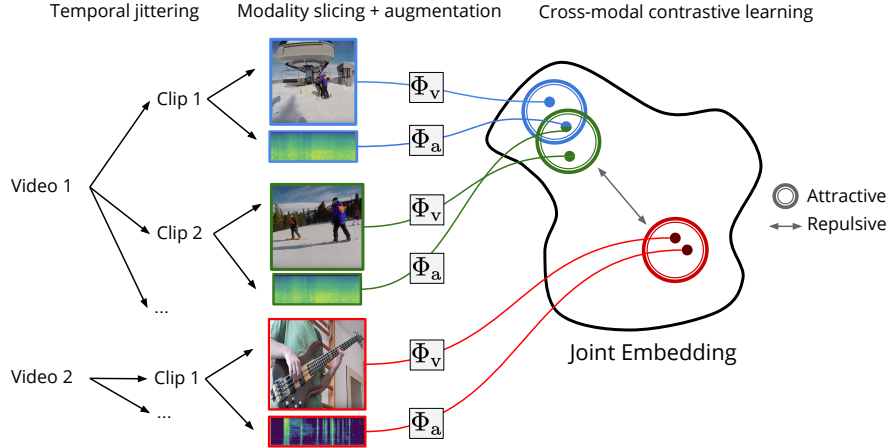


Figure 1: **Schematic overview of our GDT framework.** With GDT, the network learns a meaningful embedding via invariances across modalities and augmentations. Samples that contain the same or similar audio (e.g. from snowboarding) are learned to lie close in an embedding even though they vary in visual appearance, and vice versa. The embedding is learned via noise contrastive estimation against clips of other source videos. Illustrational videos taken from [1].

In this paper, we argue that transformations are in fact *central* to self-supervision. We develop a clear framework for semantics preserving data augmentations for multi-modal training. In particular, we view multi-modal training as a *special case* of data transformation and thus, any recent method in self-supervised learning can be applied to this case without changes.

This can be explained succinctly as follows. In self-supervision in the image domain, one starts from an image  $x$  and generates a second, congruous image  $t(x)$  by applying a nuisance transformation  $t$  to  $x$ . These transformations leave the semantic content mostly intact but can introduce noise as variance, or make the task more difficult by masking parts of the inputs. The goal is then to learn a representation  $\Phi$  which is approximately invariant to  $t$ , i.e.  $\Phi(x) \approx \Phi(t(x))$ . The latter must be paired with a constraint that the representation should also be distinctive, i.e.  $\Phi(x) \neq \Phi(x')$  if  $x$  and  $x'$  are different images.

In multi-modal learning, one starts instead from composite data  $z = (a, v)$ . For example,  $a$  could be the audio stream and  $v$  the video stream in a video. Then, instead of directly learning to predict the audio  $a$  from the video  $v$  (or vice-versa), which is an ill-posed problem, one might instead wish to learn a pair of representations  $\Phi_a(a) \approx \Phi_v(v)$ , one for each stream. In this case, distinctiveness means that  $\Phi_a(a) \neq \Phi_v(v')$  if  $(a, v) \neq (a', v')$  are two different videos.

It is then easy to combine these two approaches under the same formulation as shown in Figure 1. The first step is to consider transformations  $t(z)$  applied to the composite data. These *generalized transformations* play two roles: (a) to *slice* (selecting *which* modality to observe) and (b) to *augment* (applying a random perturbation to the modality) the data. The second step is to consider a representation  $\Phi$  that can take as input any modality. This is trivially achieved by considering a pair of networks  $\Phi = (\Phi_a, \Phi_v)$  as before, with the convention that  $\Phi(t(z))$  amounts to running either  $\Phi_a$  or  $\Phi_v$  depending on which modality is sliced by  $t$ .

Since transformations on videos can be applied in the time dimension as well, this results in a *combinatorial* space of possible transformations that can be used to slice and augment multi-modal data. A second contribution of the paper is to study this space, demonstrating the power of searching for better sets of transformations. We show empirically the power of these intuitions by building them into MoCo [19], an off-the-shelf self-supervised method for learning from static images, extending it to a state-of-the-art method for learning from multi-modal data. The resulting algorithm achieves state-of-the-art video self-supervision downstream performance for methods pretrained on the Kinetics-400 dataset [25] and even beats methods that use weak supervision such as video titles [33] for the first time.

## 2 Related work

**Early unsupervised representation learning.** Learning representations from unlabelled data has been an active area of computer vision research for decades. Early works such as auto-encoders [21], deep belief networks [22], shift-invariant decoders [48], sparse coding algorithms [31] and stacked ISAs [30] learnt image and video representations by reconstructing inputs. Recently, however, a number of works have instead focused on self-supervised learning approaches to learn representations by developing *pretext tasks* to encourage networks to learn semantics from free supervision signals available in images and videos.

**Self-supervised learning from images.** A variety of pretext tasks have been proposed to learn representations from unlabelled images. Some tasks leverage the spatial context in images [10, 39] to train CNNs. Others create pseudo classification labels by artificial rotations [14], or clustering features [6, 7, 67]. Other tasks include colorization [68, 69], predicting features [41, 20, 5], inpainting [45] and solving jigsaw puzzles [40].

**Self-supervised learning from videos.** Some of the tasks that use the space dimension of images have been extended to the space-time dimensions of videos by crafting equivalent tasks. These include predicting geometric transformations [24], jigsaw puzzles [26] and performing noise contrastive retrieval [17]. Other tasks make use of the temporal dimension of video to learn representations by predicting shuffled frames [38], the arrow of time [62], motion [60], clip order [65] or sorting sequences [32].

**Multi-modal learning.** Videos, unlike images, are a rich source of a variety of modalities such as speech, audio, and optical flow. Several works leverage the natural correspondence [3] and synchronization [28, 42] between the audio and RGB streams to learn representations. Others use a modality distillation framework to learn video [43] and sound [4] representations. With the release of the recent HowTo100M dataset [36], a large-scale instructional video dataset, a number of recent papers have leveraged speech or Automatic Speech Recognition (ASR) as a weak supervisory signal to train video representations [56, 35, 33]. These ASR models are, however, supervised models and thus implicitly contain more information than obtained from the training video datasets. Recent works have also found that multi-modal learning can lead to more robust representations as they can partly account for the different learning speeds of the different modalities [2, 64, 61].

**Noise Contrastive Loss.** Noise Contrastive losses [16] measure the similarity between sample pairs in a representational space and are at the core of several recent works on unsupervised feature learning [63, 41, 57, 19, 8]. The noise-contrastive loss function, which has recently been shown to yield good performance for images and videos [52, 19, 63, 41, 8, 35, 17, 56, 33], circumvents the need to implicitly specify what information needs to be discarded via a designed task. The combination of data augmentations and noise-contrastive re-identification is enough to train networks effectively.

Our *Generalized Data Transformations* framework contains and simplifies the recent advances in self-supervised representation learning, by extending the core idea (learning invariances from strong augmentations) from images [23, 37, 19, 11], to audio and visual streams, while naturally incorporating cross-modal and noise-contrastive training.

## 3 Method

In this section, we provide a detailed description of our proposed *Generalized Data Transformations* (GDT) learning framework. First, we discuss the motivation and formulation of our approach. Next, we describe how this can be used to train self-supervised state-of-the-art video and audio representations.

### 3.1 Semantic video transformations

**Images transformations are limited.** Transformations of the input data are key to forcing the network to learn invariances in a self-supervised setting [66]. For images, these have mostly been limited to randomly cropping and resizing [45, 68, 14, 6, 39, 40], and changes in the color histogram [57, 63, 5, 20, 13, 19, 67]. While these transformations are key for learning strong self-supervised representations for images, they do so by heavily modifying the input data distribution’s variance, which potentially affects downstream performance and still do not get close to mimicking

real 3D view changes. Furthermore, augmentations such as randomly dropping two out of three colors [45, 20] can be regarded as having more a regularizing effect and not necessarily as a content preserving transformation. Restricting oneself to data transformations that are hand-crafted and well understood (as opposed to color dropping or ones discovered by reinforcement learning, such as AutoAugment [9]) also helps understanding what invariances the network is learning.

**Video transformation are more natural.** For videos, the space for transformations is much richer due to the audio and visual stream. Crucially, videos have high frame rates of roughly 32 images per second, which allows for a large combinatorial space of cropping in time *and* space. Here, previous approaches have included randomly cropping in space and time [51, 2, 28, 17, 3, 58], and subsampling to a lower framerate [12, 2]. These transformations are relatively mild compared to those applied to images, yielding semantically strongly aligned transformations with low deviance of the real data variance. Due to the large space of transformation possibilities in time and space, even these low variance transformations can be used to train without the risk of overfitting.

On the audio stream, earlier works have only used randomly scaling the volume [3], or not augmenting the data at all [2]. In this paper, we explore the use of adding simple transformations to the audio signal. In particular, we use SpecAugment [44], which consists of masking blocks on the log mel spectrogram and was originally developed for speech recognition tasks. More specifically, SpecAugment applies random frequency masking with maximal blocking width  $f$  and sampled  $n_f$  times. Similarly, time-masking is applied with maximum width  $t$  and sampled  $n_t$  times. The masked values are set to zero and the location of the masks are sampled randomly. These transformations compensate for the faster learning speed of audio vs. video [64] and induce more robust representations from the audio encoder  $\Phi_a$ .

**Modality selection adds signal.** One simple yet effective form of transformation for inputs with multiple modalities is to select a single one. While it is more difficult to identify an action *e.g.* cutting wood without the RGB input, it should be enough to use the auditory stream alone for this task and vice versa. Incorporating this information makes the overall signal the network receives noisier, but forces the network to detect subtler differences in inputs and learn the higher level correlations.

Furthermore, when considering multi-modal tasks, the transformation space is further increased as the visual and the auditory input can be sampled at different times. There are two main ways these two signals can be temporally sampled: a) in sync: they contain the same temporal start and end points b) independent: the temporal start points are sampled independently. Notably, synchronization provides the network with additional prior knowledge that is free from the construction of the data, namely that two samples necessarily contain same semantics when they are temporally aligned.

### 3.2 Generalized Data Transformations

For training our network in a self-supervised manner, we combine the above semantic video transformations and utilize a noise contrastive loss for training.

**Loss.** Given a datapoint  $x$ , the contrastive task is defined by augmenting it with stochastic transformations  $t_i$  and detecting the correct pair of the resulting embeddings amid other samples  $x'$ , *i.e.* maximizing  $p(x|x', t_i)$ . More formally, given a network  $\Phi$ , the positive pair for datapoint  $x$  is given by  $pos(j) = \{(\Phi(t_i(x)), \Phi(t_j(x)))\}_{i,j \in \{1, \dots, T\}}$ , where  $T$  are the number of transformations applied. This formulation ensures that the method learns invariances implicit in the transformations supplied.

For computing the similarities of two samples, we keep a bank of slowly evolving features of data previously seen, following the approach of [19]. We denote  $\Phi_{ix} = \Phi(t_i(x))$  and use  $\Phi_{ix'}$  for the negative pairs.

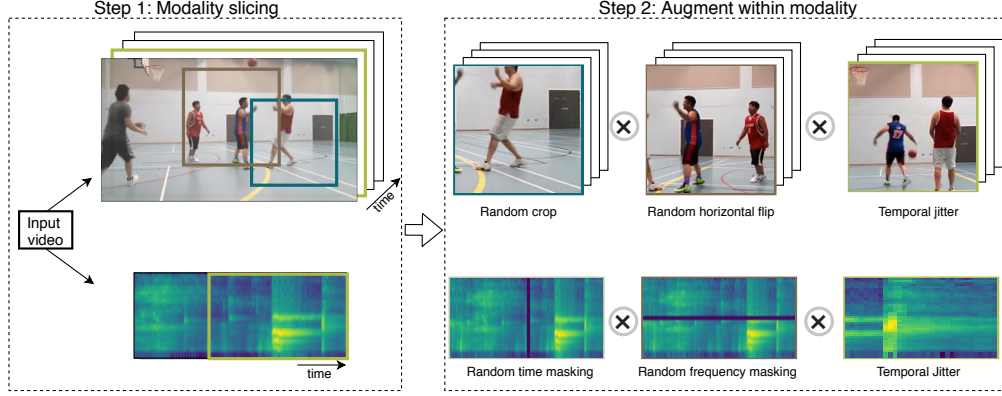


Figure 2: **GDT augmentation space for videos.** For visual clips, we apply cropping, flipping and temporal jittering. For auditory clips, we use SpecAugment [44] along with temporal jittering. In addition, both clips can be independently sampled yielding asynchronization.

With this, the loss between two positive examples is given by

$$L(x) = - \sum_{j=1}^T \sum_{i=1}^T \log p_{\Phi}(x|x', t_i, t_j) \quad (1)$$

$$= - \sum_{j=1}^T \sum_{i=1}^T \log \frac{\exp(\langle \Phi_{ix}, \Phi_{jx} \rangle_{\tau})}{\exp(\langle \Phi_{ix}, \Phi_{jx} \rangle_{\tau}) + \sum_{x'} \exp(\langle \Phi_{ix}, \Phi_{jx'} \rangle_{\tau})}, \quad (2)$$

where  $\langle \cdot, \cdot \rangle_{\tau}$  is the dot product of the L2-normalized embeddings divided by  $\tau$ , a temperature parameter for the cross entropy loss. The final loss is computed across all positive pairs with all  $N$  noise samples in the history for each datapoint  $x$  in the batch.

**Learning invariance gradually.** By writing the negative gradient of this loss with regards to the sample  $\Phi_{ix}$ , *i.e.* the direction of a step of SGD, as done in [8],

$$-\nabla_{\Phi_{ix}} L(x) \propto \Phi_{jx} (1 - \exp(2\langle \Phi_{ix}, \Phi_{jx} \rangle_{\tau})) - \sum_{\alpha=1}^N \Phi_{jx'} \exp(\langle \Phi_{ix}, \Phi_{jx'} \rangle_{\tau}), \quad (3)$$

we find that the gradient automatically reweights examples by assigning a smaller gradient to easy pairs (*i.e.*,  $\langle \Phi_{ix}, \Phi_{jx} \rangle_{\tau} \approx 1$ ) and a larger gradient to more difficult pairs. Because we use a large augmentation space that subsumes both weaker as well as stronger transformations, our method generates a curriculum implicitly: it will first learn to associate the easy pairs and then it will learn the more difficult pairs (*i.e.* heavily augmented). We confirm this hypothesis in Section 4.4.

### 3.3 Implementation for Audio-Visual Representation Learning

We use  $T = 2$ , *i.e.* work with two distinct transformations. The transformations  $t_0, t_1$ , are applied to a pair of auditory and visual inputs  $(a, v)$  and are of the form

$$t_0(a, v) = (\emptyset, t_v(v)) \quad (4)$$

$$t_1(a, v) = (t_a(a), \emptyset), \quad (5)$$

where  $t_a$  and  $t_v$  are auditory and visual transformations and  $\emptyset$  stands for the non-computation of a subspace due to slicing. Thus, dot-product similarities  $\langle \cdot, \cdot \rangle$  are only computed across modalities. Our loss thus reduces to

$$L(x) = - \log p_{\Phi}(x|x', t_a, t_v) - \log p_{\Phi}(x|x', t_v, t_a) \quad (6)$$

For  $t_a$ , we use one second clips using log mel bank features with 40 MEL filters and 99 audio frames and apply SpecAugment [44].

The visual augmentations  $t_v$  are borrowed from [28] and consist of first sampling one second of video at the original frame rate, applying a resizing to  $(128 \times 171)$ , random cropping to  $(112 \times 112)$  and random horizontal flipping. For both modalities, we explore the effect of sampling clips from the source videos at different times each epoch, which we refer to as temporal jittering. In addition, we analyze the effect of sampling the starting times independently, leading to potentially non-synchronized streams. We show examples of how these transformations affect the input in Figure 2.

As shown in [41, 57], the negative noise contrastive loss represents a lower bound on the mutual information between the two inputs  $\Phi_{i,j}$  and  $\Phi_{i+1,j}$ . With our modality-slicing transformations, minimizing the loss thus leads to increasing (a lower bound on) the mutual information between the individually augmented modalities – *i.e.* capturing the common semantics. However, optimizing an estimate of the mutual information is not a necessary condition for good representations [59].

## 4 Experiments

In this section, we provide details on our experiments. We first describe the training details and analyze our sources of gain in an ablation study. We then detail what role augmentations play in the gradual learning of invariances. Finally, we evaluate the quality of our learned representations on standardized downstream benchmark tasks.

### 4.1 Training

We pretrain our model on the GDT task on the Kinetics-400 dataset [25]. The videos in Kinetics are about 10-seconds long, each depicting one of 400 different actions. We use the training split of this dataset for pretraining ( $\approx 230\text{K}$  videos). After removing samples without audio, as in [2], we are left with around 210K videos which we use for pretraining.

We use R(2+1)-D-18 [58] as the visual encoder and ResNet-18 [18] as the audio encoder; both encoders produce a fixed-dimensional output (512-D) after global average pooling. Both vectors are then passed through a Multilayer Perceptron (MLP) head with a hidden layer size of 512 to produce 512-D embeddings which are normalized by their L2-norm [63]. The MLP embedding is used for computing the contrastive loss, while for downstream tasks, a linear layer after the global average pooling is used. For contrastive learning, the temperature  $\tau$  is set as 0.07, memory bank size as 15000, momentum update parameter as 0.999 and we use shuffling of the batchnorm statistics, closely following the parameters of [19]. For optimizing these networks, we use SGD. The SGD weight decay is  $10^{-5}$  and the SGD momentum is 0.9. We use a mini-batch size of 16 on each of our 64 GPUs giving an effective batch size of 1024 for distributed training. The initial learning rate is set to 0.01 which we linearly scale with the number of GPUs, after following a gradual warm-up schedule for the first 10 epochs [15]. We train for 200 epochs overall except in our ablations, where we train for 100 epochs.

### 4.2 Evaluation on Downstream Tasks

**Action Recognition.** We evaluate our learned video representations on the medium-sized action recognition benchmark datasets UCF101 [53] and HMDB51 [29]. UCF101 contains about 13K videos from 101 human action classes, and HMDB51 consists of 7K clips spanning 51 different human activities.

To evaluate the learned video representations, we finetune our pretrained network. During training, we take 10 random clips of length 30 frames from each video. For video clip augmentations, we follow a standard protocol as in [28], see Appendix for details. During evaluation, we uniformly sample 10 clips from each video, average softmax scores, and predict the class having the highest mean softmax score. We then measure the mean video top-1 accuracy across all videos and all official folds.

**Audio Event Classification.** We evaluate our learned audio representations on ESC-50 [47] and DCASE2014 [54]. ESC-50 is an environmental sound classification dataset which has 2K clips of

(a) **Temporal jittering (TJ).**

TJ	UCF		HMDB	
	50	100	50	100
✗	73.1	71.2	42.7	44.4
✓	<u>82.3</u>	<u>86.1</u>	<u>49.4</u>	<u>54.3</u>

(b) **Audio augmentation and synchronization.**

SA	sync?	UCF		HMDB	
		50	100	50	100
no	✗	77.7	83.2	45.2	50.2
no	✓	82.3	86.1	49.4	54.3
mild	✓	81.5	86.1	<u>51.4</u>	54.7
strong	✓	<u>82.7</u>	<u>86.5</u>	49.7	<u>56.0</u>

Table 1: **Ablation studies.** For these experiments we report Top-1 accuracies in % for two video classification downstream tasks, see Appendix for details.

50 different audio classes. DCASE2014 is an acoustic scenes and event classification dataset which has 100 training clips of 10 different audio classes.

For audio feature evaluation, we follow the protocol of [28] and do *not* finetune the audio network. We extract 10 equally spaced 2-second sub-clips from each full audio sample of ESC-50 [47] and train a L2 regularized linear layer on the audio network’s max-pooled *conv5* features, see Appendix for details. For DCASE2014 [54], we extract 60 1-second sub-clips from each full sample and directly train a multiclass one-vs-all linear SVM to classify the audio events. The classification score for each audio sample is computed by averaging the sub-clip scores in the sample, and then predicting the class with the highest score. The mean top-1 accuracy is then taken across all audio clips and averaged across all official folds.

### 4.3 Analysis of Transformations

From Table 1(a), we find that temporal jittering (TJ) is essential when training neural networks in a self-supervised fashion. While the self-supervision losses keep decreasing, we find that the downstream task performance quickly saturates at around epoch 100 when not using TJ. This overfitting phenomenon is somewhat surprising as the space of possible random-cropped locations is still very large and indeed is the standard for image level self-supervision. This shows that increasing the amount of data points, even if they come from the same source video, is a clear way to enhance performance. In particular, here we increase downstream task performance by more than 8% on both datasets. This result presents a complementary insight to the recent gains in video representation learning that show large gains from using  $10\times$  to  $150\times$  more data [28, 2, 4].

From Table 1(b), we find that injecting prior information into the network training helps learn more generalizable representations. This insight is drawn firstly from the fact that we increase the performance by more than 3% by using synchronized temporal jittering. In contrast to setting positive pairs as non-synchronized subclips, synchronization facilitates the learning of representations that are distinct in the temporal dimension due to the contrastive loss. Furthermore, we find that adding simple audio augmentations that do not change the semantics, via SpecAugment (SA), can further increase the performance. Here, we explore the effect of a mild set of augmentation parameters ( $n_f = 1$ ,  $f = 2$ ,  $n_t = 1$  and  $t = 5$ .) and a stronger one ( $n_f = 2$ ,  $f = 3$ ,  $n_t = 2$  and  $t = 6$ .) and find that we can increase performance by another 1.7% for HMDB51 and 0.4% for UCF101 compared to not augmenting. The augmentations aid the downstream task performance as they require learning more stable representations in the audio space which in turn increase the performance of the visual embedding due to our modality slicing transformations.

### 4.4 Analysis of a Natural Curriculum

We analyze the times at which the networks learn to become invariant to which type of augmentations. For this, in Figure 3, we plot the contrastive re-identification top-1 accuracies for various strengths of augmentations against network training time. We find that the network’s accuracy rises sharpest for the samples that are only randomly cropped. For samples with stronger augmentations, we see that its learning speed lags behind, and thus yielding a natural curriculum-type learning when combined with the contrastive loss.

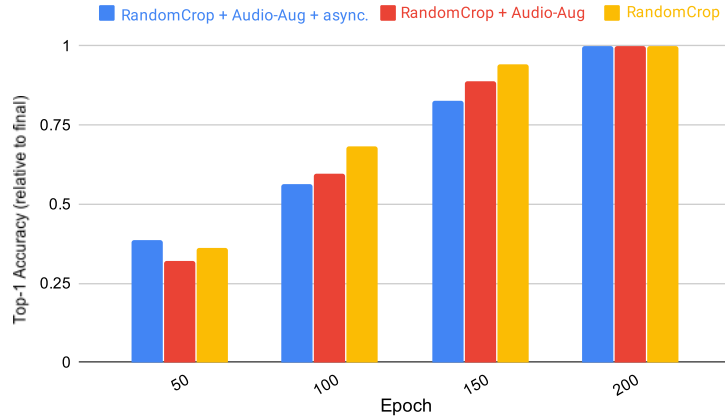


Figure 3: **Natural curriculum.** We show the relative noise contrastive re-identification accuracy against training time. Lightly augmented data samples are learned first.

Method	Architecture	Pretrain Dataset	Top-1 Acc%	
			UCF	HMDB
Full supervision	R(2+1)D-18	ImageNet	82.8	46.7
Full supervision	R(2+1)D-18	Kinetics-400	<u>93.1</u>	<u>63.6</u>
Weak supervision, CPD [33]	3D-Resnet50	Kinetics-400 <sup>†</sup>	88.7	57.7
Shuffle&Learn [38]	CaffeNet	UCF/HMDB	50.2	18.1
OPN [32]	VGG	UCF/HMDB	-	23.8
ClipOrder [65]	R(2+1)D-18	UCF	-	30.9
MotionPred [60]	C3D	Kinetics-400	61.2	33.4
RotNet3D [24]	3D-ResNet18	Kinetics-600	62.9	33.7
ST-Puzzle [26]	3D-ResNet18	Kinetics-400	65.8	33.7
DPC [17]	3D-ResNet34	Kinetics-400	75.7	35.7
CBT [56]	S3D	Kinetics-600	79.5	44.6
Multisensory [42]	3D-ResNet18	Kinetics-400	82.1	-
XDC [2]	R(2+1)D-18	Kinetics-400	84.2	47.1
AVTS [28]	MC3-18	Kinetics-400	85.8	56.9
AV Sync+RotNet [64]	AVSlowFast	Kinetics-400	87.0	54.6
<b>GDT (ours)</b>	R(2+1)D-18	Kinetics-400	<b>88.7</b>	<b>57.8</b>

Table 2: **State-of-the-art on video action recognition.** Self-supervised and fully-supervised trained methods on UCF101 and HMDB51 benchmarks. We report the average top-1 accuracy over the official splits. We report results for finetuning the whole network. Methods with <sup>†</sup> indicate the additional use of video titles and ASR generated text as supervision. See Table A.1 in the Appendix for a full version of this table including models trained with much larger datasets.

#### 4.5 Comparison to state of the art

**Video Action Recognition.** Table 2 compares GDT pretrained on Kinetics-400 against state-of-the-art self-supervised methods, after finetuning on the UCF101 and HMDB51 benchmarks. We also compare against two fully-supervised methods pretrained on ImageNet and Kinetics and then finetuned on UCF101 and HMDB51. When constrained to pretraining on the Kinetics datasets, we find that our model with the GDT framework achieves state-of-the-art results among all self-supervised approaches on both downstream action recognition datasets. As the next best method, AudioVisual SlowFast networks [64], reaches close performance only by applying a more advanced architecture and combining two losses. We expect our method to yield even better results when combined with stronger architectures, as combining tasks has been shown to improve feature learning performance in multiple other papers [10, 67, 13]. Finally, we observe that our GDT trained model also surpasses



Method	Pre-training		Top-1 Acc%	
	Dataset	#data	DCASE	ESC-50
Autoencoder [4]	SoundNet	2M+	-	39.9
Random Forest [47]	ESC-50	1.6K	-	44.3
Piczak ConvNet [46]	ESC-50	1.6K	-	64.5
RNH [49]	DCASE2014	100	72	-
Ensemble [55]	DCASE2014	100	77	-
AVTS [28]	Kinetics-400	230K	<u>91</u>	76.7
XDC [2]*	Kinetics-400	230K	-	78.0
ConvRBM [50]	ESC-50	1.6K	-	<b>86.5</b>
<b>GDT (ours)</b>	Kinetics-400	230K	<b>94</b>	<u>78.6</u>
<i>Using larger datasets</i>				
SoundNet [4]	SoundNet	2M+	<b>88</b>	74.2
L3-Net [3]	SoundNet	2M+	93	79.3
AVTS [28]	SoundNet	2M+	94	82.3
XDC [2]	AudioSet	1.8M	93	84.8

Table 3: **Audio event classification.** Downstream task top-1 accuracies on standard audio classification benchmarks after finetuning. Methods with \* use full-finetuning of their encoder network.

the CPD [33] method on HMDB which uses ASR generated text scripts along with weak supervision of video titles for pretraining a network.

**Audio Event Classification.** Table 3 compares GDT pretrained on Kinetics-400 against other methods for the downstream tasks of audio classification on the DCASE2014 and ESC-50 datasets. For DCASE2014, we reach state-of-the-art performance that only one other method (AVTS) reaches with an almost  $10\times$  larger dataset. Using the same pretraining, AVTS reports 91% accuracy, showing that a larger part of the gain is due to dataset size. Similarly, on ESC-50, our method outperforms AVTS pretrained on the Kinetics-400 by almost 2% and even surpasses the performance of XDC with finetuning of the whole encoder network, as well as SoundNet which was trained on a much larger and more diverse dataset [4].

## 5 Conclusion

In this work, we have introduced a framework for data transformations in a multi-modal setting that encompasses recent advances in self-supervised learning of images and videos. We argue that transformations, often only mentioned in the appendices of papers, deserve a more prominent place in the field of video representation learning because they are key to constructing strong content preserving augmentations of the data that induce valuable invariances. By means of ablations, we validate that our Generalized Data Transformation framework is well suited for training representations in a self-supervised manner when combined with a contrastive training loss and report state-of-the-art results as pretraining for standard downstream tasks.

## Acknowledgments and Disclosure of Funding

We are grateful for support from the Rhodes Trust (M.P.), Facebook (M.P.), EPSRC Centre for Doctoral Training in Autonomous Intelligent Machines & Systems [EP/L015897/1] (M.P. and Y.A.), the Open Philanthropy Project (R.F.), and the Royal Academy of Engineering under the Research Fellowship scheme (J.F.H.). We also thank Andrew Owens, Alexei Efros and Tengda Han for helpful discussions on self-supervised learning. Lastly, the authors would also like to thank Ishan Misra and Bruno Korbar from Facebook for valuable discussions and sharing insights.

## References

- [1] <https://youtu.be/-Wr6W0Xnztk>, <https://youtu.be/-BmuSpck3U>.
- [2] Humam Alwassel, Dhruv Mahajan, Lorenzo Torresani, Bernard Ghanem, and Du Tran. Self-supervised learning by cross-modal audio-video clustering. *arXiv preprint arXiv:1911.12667*, 2019.
- [3] Relja Arandjelović and Andrew Zisserman. Look, listen and learn. In *ICCV*, 2017.
- [4] Yusuf Aytar, Carl Vondrick, and Antonio Torralba. Soundnet: Learning sound representations from unlabeled video. In *NeurIPS*, 2016.
- [5] Philip Bachman, R Devon Hjelm, and William Buchwalter. Learning representations by maximizing mutual information across views, 2019.
- [6] Mathilde Caron, Piotr Bojanowski, Armand Joulin, and Matthijs Douze. Deep clustering for unsupervised learning of visual features. In *ECCV*, 2018.
- [7] Mathilde Caron, Piotr Bojanowski, Julien Mairal, and Armand Joulin. Unsupervised pre-training of image features on non-curated data. In *ICCV*, 2019.
- [8] Ting Chen, Simon Kornblith, Mohammad Norouzi, and Geoffrey E. Hinton. A simple framework for contrastive learning of visual representations. *ArXiv*, abs/2002.05709, 2020.
- [9] Ekin D Cubuk, Barret Zoph, Dandelion Mane, Vijay Vasudevan, and Quoc V Le. Autoaugmentation: Learning augmentation strategies from data. In *Proceedings of the IEEE conference on computer vision and pattern recognition*, pages 113–123, 2019.
- [10] Carl Doersch, Abhinav Gupta, and Alexei A Efros. Unsupervised visual representation learning by context prediction. In *ICCV*, 2015.
- [11] Alexey Dosovitskiy, Philipp Fischer, Jost Tobias Springenberg, Martin Riedmiller, and Thomas Brox. Discriminative unsupervised feature learning with exemplar convolutional neural networks. *TPAMI*, 38(9), 2015.
- [12] Christoph Feichtenhofer, Haoqi Fan, Jitendra Malik, and Kaiming He. Slowfast networks for video recognition. In *ICCV*, 2019.
- [13] Zeyu Feng, Chang Xu, and Dacheng Tao. Self-supervised representation learning by rotation feature decoupling. In *The IEEE Conference on Computer Vision and Pattern Recognition (CVPR)*, June 2019.
- [14] Spyros Gidaris, Praveer Singh, and Nikos Komodakis. Unsupervised representation learning by predicting image rotations. *ICLR*, 2018.
- [15] Priya Goyal, Piotr Dollár, Ross Girshick, Pieter Noordhuis, Lukasz Wesolowski, Aapo Kyrola, Andrew Tulloch, Yangqing Jia, and Kaiming He. Accurate, large minibatch SGD: training imagenet in 1 hour. *arXiv preprint arXiv:1706.02677*, 2017.
- [16] Raia Hadsell, Sumit Chopra, and Yann LeCun. Dimensionality reduction by learning an invariant mapping. *Proc. CVPR*, 2:1735–1742, 2006.
- [17] Tengda Han, Weidi Xie, and Andrew Zisserman. Video representation learning by dense predictive coding. In *ICCV*, 2019.
- [18] Kaiming He, Xiangyu Zhang, Shaoqing Ren, and Jian Sun. Deep residual learning for image recognition. In *CVPR*, 2016.
- [19] Kaiming He, Haoqi Fan, Yuxin Wu, Saining Xie, and Ross Girshick. Momentum contrast for unsupervised visual representation learning, 2019.
- [20] Olivier J Hénaff, Ali Razavi, Carl Doersch, SM Eslami, and Aaron van den Oord. Data-efficient image recognition with contrastive predictive coding. *arXiv preprint arXiv:1905.09272*, 2019.

- [21] Geoffrey E Hinton and Ruslan R Salakhutdinov. Reducing the dimensionality of data with neural networks. *Science*, 2006.
- [22] Geoffrey E Hinton, Simon Osindero, and Yee-Whye Teh. A fast learning algorithm for deep belief nets. *Neural computation*, 2006.
- [23] Xu Ji, João F. Henriques, and Andrea Vedaldi. Invariant information clustering for unsupervised image classification and segmentation, 2018.
- [24] Longlong Jing and Yingli Tian. Self-supervised spatiotemporal feature learning by video geometric transformations. *arXiv preprint arXiv:1811.11387*, 2018.
- [25] Will Kay, Joao Carreira, Karen Simonyan, Brian Zhang, Chloe Hillier, Sudheendra Vijayanarasimhan, Fabio Viola, Tim Green, Trevor Back, Paul Natsev, Mustafa Suleyman, and Andrew Zisserman. The kinetics human action video dataset. *CoRR*, abs/1705.06950, 2017.
- [26] Dahun Kim, Donghyeon Cho, and In So Kweon. Self-supervised video representation learning with space-time cubic puzzles. In *AAAI*, 2019.
- [27] Diederik P. Kingma and Jimmy Ba. Adam: A method for stochastic optimization. In *ICLR*, 2015.
- [28] Bruno Korbar, Du Tran, and Lorenzo Torresani. Cooperative learning of audio and video models from self-supervised synchronization. In *NeurIPS*, 2018.
- [29] Hildegard Kuehne, Hueihan Jhuang, Estíbaliz Garrote, Tomaso Poggio, and Thomas Serre. HMDB: a large video database for human motion recognition. In *ICCV*, 2011.
- [30] Quoc V Le, Will Y Zou, Serena Y Yeung, and Andrew Y Ng. Learning hierarchical invariant spatio-temporal features for action recognition with independent subspace analysis. In *CVPR*, 2011.
- [31] Honglak Lee, Alexis Battle, Rajat Raina, and Andrew Y Ng. Efficient sparse coding algorithms. In *NeurIPS*, 2007.
- [32] Hsin-Ying Lee, Jia-Bin Huang, Maneesh Singh, and Ming-Hsuan Yang. Unsupervised representation learning by sorting sequences. In *ICCV*, 2017.
- [33] Tianhao Li and Limin Wang. Learning spatiotemporal features via video and text pair discrimination, 2020.
- [34] David G. Lowe. Distinctive image features from scale-invariant keypoints. *Int. J. Comput. Vision*, 60(2):91–110, November 2004.
- [35] Antoine Miech, Jean-Baptiste Alayrac, Lucas Smaira, Ivan Laptev, Josef Sivic, and Andrew Zisserman. End-to-end learning of visual representations from uncurated instructional videos, 2019.
- [36] Antoine Miech, Dimitri Zhukov, Jean-Baptiste Alayrac, Makarand Tapaswi, Ivan Laptev, and Josef Sivic. Howto100M: Learning a text-video embedding by watching hundred million narrated video clips. In *ICCV*, 2019.
- [37] Ishan Misra and Laurens van der Maaten. Self-supervised learning of pretext-invariant representations, 2019.
- [38] Ishan Misra, C Lawrence Zitnick, and Martial Hebert. Shuffle and learn: unsupervised learning using temporal order verification. In *ECCV*, 2016.
- [39] Mehdi Noroozi and Paolo Favaro. Unsupervised learning of visual representations by solving jigsaw puzzles. In *ECCV*, 2016.
- [40] Mehdi Noroozi, Hamed Pirsiavash, and Paolo Favaro. Representation learning by learning to count. In *ICCV*, 2017.

- [41] Aaron van den Oord, Yazhe Li, and Oriol Vinyals. Representation learning with contrastive predictive coding. *arXiv preprint arXiv:1807.03748*, 2018.
- [42] Andrew Owens and Alexei A Efros. Audio-visual scene analysis with self-supervised multi-sensory features. In *ECCV*, 2018.
- [43] Andrew Owens, Jiajun Wu, Josh H McDermott, William T Freeman, and Antonio Torralba. Ambient sound provides supervision for visual learning. In *ECCV*, 2016.
- [44] Daniel S. Park, William Chan, Yu Zhang, Chung-Cheng Chiu, Barret Zoph, Ekin D. Cubuk, and Quoc V. Le. Specaugment: A simple data augmentation method for automatic speech recognition. *Interspeech 2019*, Sep 2019.
- [45] Deepak Pathak, Philipp Krahenbuhl, Jeff Donahue, Trevor Darrell, and Alexei A Efros. Context encoders: Feature learning by inpainting. In *CVPR*, 2016.
- [46] Karol J. Piczak. Environmental sound classification with convolutional neural networks. *MLSP*, 2015.
- [47] Karol J. Piczak. Esc: Dataset for environmental sound classification. In *ACM Multimedia*, 2015.
- [48] Marc’auelio Ranzato, Fu Jie Huang, Y-Lan Boureau, and Yann LeCun. Unsupervised learning of invariant feature hierarchies with applications to object recognition. In *CVPR*, 2007.
- [49] Guido Roma, Waldo Nogueira, and Perfecto Herrera. Recurrence quantification analysis features for environmental sound recognition. *WASPAA*, 2013.
- [50] Hardik B. Sailor, Dharmesh M Agrawal, and Hemant A Patil. Unsupervised filterbank learning using convolutional restricted boltzmann machine for environmental sound classification. In *INTERSPEECH*, 2017.
- [51] Karen Simonyan and Andrew Zisserman. Two-stream convolutional networks for action recognition in videos. In *ICLR*, pages 568–576, 2014.
- [52] Kihyuk Sohn. Improved deep metric learning with multi-class n-pair loss objective. In *Proc. NIPS*, pages 1857–1865, 2016.
- [53] Khurram Soomro, Amir Roshan Zamir, and Mubarak Shah. UCF101: A dataset of 101 human actions classes from videos in the wild. *arXiv preprint arXiv:1212.0402*, 2012.
- [54] D. Stowell, D. Giannoulis, E. Benetos, M. Lagrange, and M. D. Plumbley. Detection and classification of acoustic scenes and events. *IEEE Transactions on Multimedia*, 17(10):1733–1746, Oct 2015. ISSN 1520-9210. doi: 10.1109/TMM.2015.2428998.
- [55] Dan Stowell, Dimitrios Giannoulis, Emmanouil Benetos, Mathieu Lagrange, and Mark D. Plumbley. Detection and classification of acoustic scenes and events. *TM*, 2015.
- [56] Chen Sun, Fabien Baradel, Kevin Murphy, and Cordelia Schmid. Contrastive bidirectional transformer for temporal representation learning. *arXiv preprint arXiv:1906.05743*, 2019.
- [57] Yonglong Tian, Dilip Krishnan, and Phillip Isola. Contrastive multiview coding. *arXiv preprint arXiv:1906.05849*, 2019.
- [58] Du Tran, Heng Wang, Lorenzo Torresani, Jamie Ray, Yann LeCun, and Manohar Paluri. A closer look at spatiotemporal convolutions for action recognition. In *CVPR*, 2018.
- [59] Michael Tschannen, Josip Djolonga, Paul K. Rubenstein, Sylvain Gelly, and Mario Lucic. On mutual information maximization for representation learning. In *Proc. ICLR*, 2020.
- [60] Jiangliu Wang, Jianbo Jiao, Linchao Bao, Shengfeng He, Yunhui Liu, and Wei Liu. Self-supervised spatio-temporal representation learning for videos by predicting motion and appearance statistics. In *CVPR*, 2019.

- [61] Weiyao Wang, Du Tran, and Matt Feiszli. What makes training multi-modal classification networks hard?, 2019.
- [62] Donglai Wei, Joseph J Lim, Andrew Zisserman, and William T Freeman. Learning and using the arrow of time. In *CVPR*, 2018.
- [63] Zhirong Wu, Yuanjun Xiong, Stella X. Yu, and Dahua Lin. Unsupervised feature learning via non-parametric instance discrimination. In *Proc. CVPR*, June 2018.
- [64] Fanyi Xiao, Yong Jae Lee, Kristen Grauman, Jitendra Malik, and Christoph Feichtenhofer. Audiovisual slowfast networks for video recognition, 2020.
- [65] Dejing Xu, Jun Xiao, Zhou Zhao, Jian Shao, Di Xie, and Yueting Zhuang. Self-supervised spatiotemporal learning via video clip order prediction. In *CVPR*, 2019.
- [66] Asano YM., Rupprecht C., and Vedaldi A. A critical analysis of self-supervision, or what we can learn from a single image. In *International Conference on Learning Representations*, 2020.
- [67] Asano YM., Rupprecht C., and Vedaldi A. Self-labelling via simultaneous clustering and representation learning. In *Proc. ICLR*, 2020.
- [68] Richard Zhang, Phillip Isola, and Alexei A Efros. Colorful image colorization. In *ECCV*, 2016.
- [69] Richard Zhang, Phillip Isola, and Alexei A Efros. Split-brain autoencoders: Unsupervised learning by cross-channel prediction. In *Proc. CVPR*, 2017.

## A Appendix

### A.1 Ablation experiment details

For the ablations, we only train for 100 epochs unless specified otherwise. For subtable (a), we use the synchronized version without any audio augmentation and use 15K negatives. For both downstream tasks, we only evaluate on the first fold each but found the performance between folds to be close (within 1-2%).

### A.2 Finetuning details

**Video** We use SGD with initial learning rate 0.0025, which we gradually warm up to  $2 \cdot 10^{-2}$  in the first 2 epochs. The weight decay is set to  $5 \cdot 10^{-3}$  and momentum to 0.9. We use a mini-batch size of 32 and train for 10 epochs with the learning rate multiplied by  $1 \cdot 10^{-2}$  at 6 and 8 epochs.

**Audio** For both tasks, we save the activations that result from the audio encoder to quickly train the linear classifiers. We use activations after the last convolutional layer of the ResNet-18 and apply a max pooling with kernelsize (1,3) and stride of (1,2) without padding to the output. For ESC-50, we then optimize a L2 regularized linear layer with batch size 512 using the Adam optimizer [27] with learning rate  $1 \cdot 10^{-4}$ , weight-decay set to  $5 \cdot 10^{-4}$  and the default parameters. For DCASE2014, we train a linear SVM with  $C = 0.01$ , and without using the dual in the optimization (it yields the same results).

Method	Architecture	Pretrain Dataset	Top-1 Acc%	
			UCF	HMDB
Full supervision	R(2+1)D-18	ImageNet	82.8	46.7
Full supervision	R(2+1)D-18	Kinetics-400	<u>93.1</u>	<u>63.6</u>
Weak supervision, CPD [33]	3D-Resnet50	Kinetics-400 <sup>†</sup>	88.7	57.7
Shuffle&Learn [38]	CaffeNet	UCF/HMDB	50.2	18.1
OPN [32]	VGG	UCF/HMDB	-	23.8
ClipOrder [65]	R(2+1)D-18	UCF	-	30.9
MotionPred [60]	C3D	Kinetics-400	61.2	33.4
RotNet3D [24]	3D-ResNet18	Kinetics-600	62.9	33.7
ST-Puzzle [26]	3D-ResNet18	Kinetics-400	65.8	33.7
DPC [17]	3D-ResNet34	Kinetics-400	75.7	35.7
CBT [56]	S3D	Kinetics-600	79.5	44.6
Multisensory [42]	3D-ResNet18	Kinetics-400	82.1	-
XDC [2]	R(2+1)D-18	Kinetics-400	84.2	47.1
AVTS [28]	MC3-18	Kinetics-400	85.8	56.9
AV Sync+RotNet [64]	AVSlowFast	Kinetics-400	87.0	54.6
<b>GDT (ours)</b>	R(2+1)D-18	Kinetics-400	<b>88.7</b>	<b>57.8</b>
<i>Using larger datasets</i>				
L <sup>3</sup> -Net [3]	VGG	AudioSet	72.3	40.2
AVTS [28]	MC3-18	AudioSet	89.0	<b>61.6</b>
XDC [2]	R(2+1)D-18	AudioSet	91.2	61.0
MIL-NCE [35]	S3D	HowTo100M*	<b>91.3</b>	61.0

Table A.1: **State-of-the-art on video action recognition.** Self-supervised and fully-supervised trained methods on UCF101 and HMDB51 benchmarks. We report the average top-1 accuracy over the official splits. We report results for finetuning the whole network. Methods with <sup>†</sup> indicate the additional use of video titles and ASR generated text as supervision. Methods with \* use ASR generated text.